2014 IEEE International Conference on Robotics & Automation (ICRA)
Hong Kong Convention and Exhibition Center
May 31 - June 7, 2014. Hong Kong, China

A Three-Axial Body Force Sensor for Flexible Manipulators

Yohan Noh, Sina Sareh, Jungwhan Back, Helge A Würdemann, Tommaso Ranzani, Emanuele Lindo Secco, Angela Faragasso, Hongbin Liu, *IEEE Member*, Kaspar Althoefer, *IEEE Member*

***Abstract*— This paper introduces an optical based three axis force sensor which can be integrated with the robot arm of the EU project STIFF-FLOP (STIFFness controllable Flexible and Learnable Manipulator for Surgical Operations) in order to measure applied external forces. The structure of the STIFF-FLOP arm is free of metal components and electric circuits and, hence, is inherently safe near patients during surgical operations. In addition, this feature makes the performance of this sensing system immune against strong magnetic fields inside magnetic resonance (MR) imaging scanners. The hollow structure of the sensor allows the implementation of distributed actuation and sensing along the body of the manipulator. In this paper, we describe the design and calibration procedure of the proposed three axis optics-based force sensor. The experimental results confirm the effectiveness of our optical sensing approach and its applicability to determine the force and momentum components during the physical interaction of the robot arm with its environment.**

I. Introduction

Using Robot Technology, minimally invasive surgery (MIS) has considerably advanced over the last few decades. Recently, robotic surgical devices such as da Vinci surgery system take advantages of cutting edge robot technology leading to tremendous advancement in stable and safe MIS. Such surgical devices enable doctors to perform surgical operation precisely making use of the feedback from vision systems - 3D surgical cameras are employed enhancing the doctors' performance during complex surgery in confined spaces. Employing these stable, tremor-free and intuitive surgical systems, operations are tremendously simplified when compared to standard laparoscopy [1-2].

However, due to their rigid structure and the low degrees of freedom, such medical devices require a large motion workspace to perform surgical operations. These devices have limited ability to pass and maneuver inside small openings and confined spaces. Moreover, they do not use tactile and force sensors, and therefore are not able to protect delicate internal organs. As a result, these robotic systems can cause patients to be in a critical condition during or after the operation.

In order to overcome the shortcomings of the conventional, rigid medical devices, researchers have started to develop flexible manipulators. Taylor et al. developed a flexible snake-like manipulator that can demonstrate high degrees of actuation dexterity in confined spaces [3-4]. However this device is not capable of changing its stiffness. Simaan et al. also proposed a dexterous, flexible manipulator, which can articulate into complex shapes [5-6]. Active cannulas manipulators by Webster et al. are a new class of thin, dexterous continuum robots that can access narrow openings such as the throat and lung [7-8]. Cheng et al. developed a flexible manipulator, which can change its stiffness and is capable of dexterous precise motion control using cables [9]. Another flexible and stiffness-controllable robot concept was introduced by Jiang et al. [10-11]. However, the above manipulators are not equipped with any tactile/force sensors inside or outside of the manipulator structure and, thus,

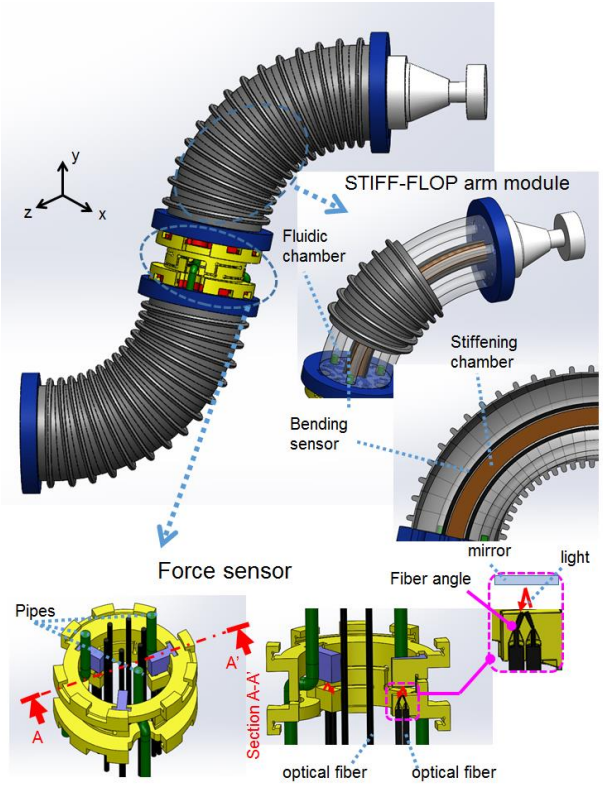

Figure 1. Overview of the STIFF-FLOP manipulator and three axis sensor

Manuscript received Feb 15th, 2014. The research leading to these results has received funding from the European Commission's Seventh Framework Programme; project STIFF-FLOP (Grant No: 287728).

Yohan Noh, Sina Sareh, Jungwhan Back, Würdemann Helge, Emanuele Lindo Secco, Angela Faragasso, Hongbin Liu, and Kaspar Althoefer are with Centre of Robotics Research, King's College London, School of Natural and Mathematical Sciences, Department of Informatics, UK (e-mail corresponding author: yohan.noh@kcl.ac.uk).

Tommaso Ranzani is with Scuola Superiore Sant'Anna, The BioRobotics Institute, Italy

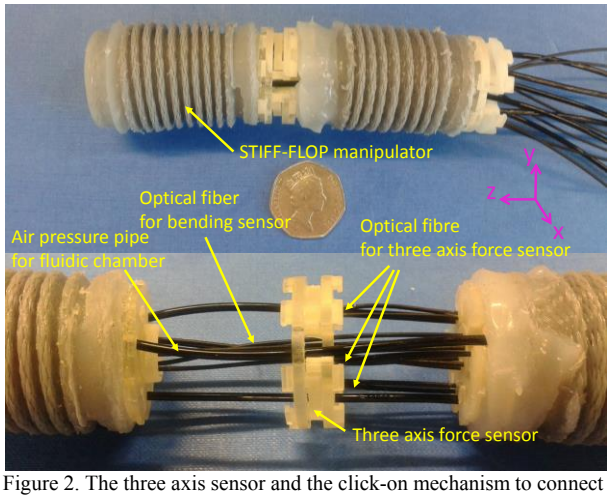

Figure 2. The three axis sensor and the click-on mechanism to connect with the STIFF-FLOP manipulator

cannot provide force feedback to the surgeon.

For these reasons, we have been developing a multi-DoF force sensor for the arm of the EU-project STIFF-FLOP, in collaboration with 11 European academic partners (www.stiff-flop.eu) [12-14]. The STIFF-FLOP arm is a soft robotic arm that can squeeze through standard MIS trocar ports enabling precise closed-loop motion control of the arm, i.e. omni-elongation and bending of the arm using air pressure feedback and bending sensors [15] (a sketch of the arm is shown in Fig 1). In addition, the stiffness of the arm can be adjusted at various regions along its length through granular jamming [10-11]. This provides opportunities to perform compliant force control tasks using force and tactile sensors while the robot is moving through the abdominal environment of a patient. Moreover, due to the lack of metal components and electric circuits in the structure of the STIFF-FLOP arm, the surgical operation can be potentially carried out employing intra-operative MRI (Magnetic Resonance Imaging).

Conventional multi axial force sensors usually employ strain gauges driven by electrical circuitry and are made of metal components. The application of this class of sensors makes the robotic system vulnerable to magnetic or electrical fields. Also, these sensors usually do not have a hollow structure and, thus, prevent the passing through of cables and tubes that may be needed for a fully-functional surgical device. Often the standard force sensors do not conform to the geometry of the STIFF-FLOP arm. Hence, to enable embodiment of the multi-axis force sensor along with other actuation and sensing components, and to preserve unique advantages of the STIFF-FLOP arm including MR compatibility, a new sensor approach was explored here.

To tackle the aforementioned limitations, we take advantage of a fiber optic sensing approach [16-19], which is inherently safe and well-suited to be accompanied with intra-operative imaging systems [18]. Here, a ring-shaped multi-axis force sensor, as shown in Figs. 1 and 2, is designed and implemented allowing actuation and sensing components of the arm to pass through from the base of robot to its tip, including the pipes for the fluidic actuation chambers to pass

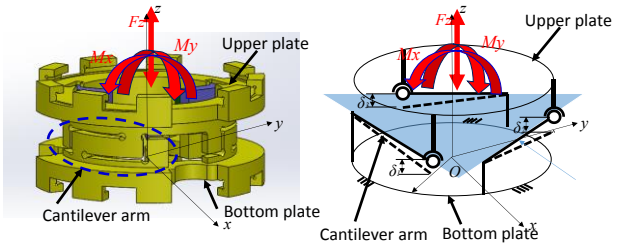

Figure 3. Equivalent spring model of the flexible tripod platform

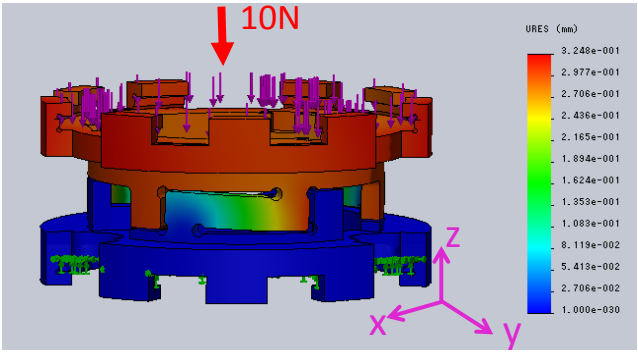

Figure 4. FEM Simulation performed with the Solidworks Simulation tool

between successive segments of the manipulator.

In this paper, we present the design and development of an optical based three axis force sensor which can measure applied forces. In the following text, we explain the design, calibration, and calculation of the force components of the sensor. Finally, from the result of the experiments, we verify our proposed methods.

II. Design Methods and Fabrication

A. Design Concept

The design concept of the multi axial force sensor should satisfy several conditions as follows:

1) The sensor employs optical fiber technology to be immune against magnetic and electric fields. Also, our approach eliminates possible damage to the patients due to electric currents.

2) This sensor devices will also serve as connecting element between segments of the STIFF-FLOP manipulator and, hence, should have a ring-like structure to conform to the shape of the manipulator. A hollow section in the central region of the sensor should be provided to allow auxiliary pipes and cables to pass through.

3) The sensor should be capable of measuring three components of external force and moments including F_z, M_x, and M_y in order to determine relevant interactions with the environment. Note that, the STIFF-FLOP manipulator has 3 DoF including two omni-directional bending motions and an elongation motion.

B. Configuration of Optical Multi Axial Force Sensor

The structure of optical three axis force sensor is shown in Figs. 1 and 2. The sensor uses quarter millimeter thick optical fibers SH1001-1.0 from LasIRvis Co. Ltd, mirrors as reflective surfaces, and a flexible ring-like structure to

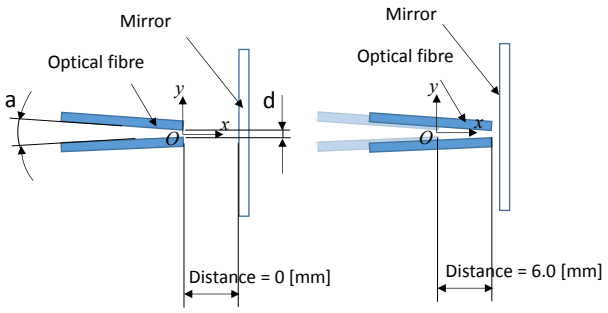

Figure 5. Experiment setup of the optical fibres

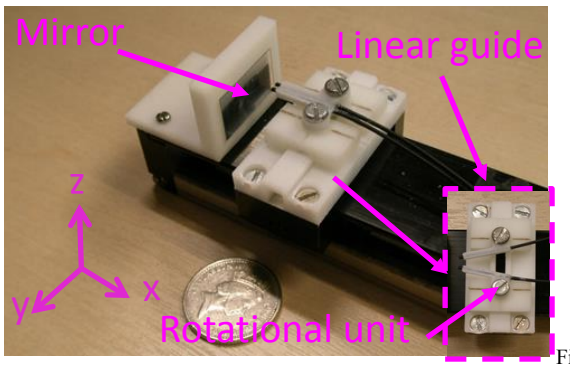

Figure 6. Configuration of the device for the optimization of the fibers' configuration

measure a force component F_z and two moment components, M_x and M_y. In order to measure these three force and moment components, at least three deformations of the sensor's structure need to be measured, as illustrated in Fig. 3

The sensor makes use of a pair of optical fibers, one of them used for emitting the light and the other one for the receiving the light [16-19]. Fibers are arranged at a specific angle with respect to each other, as shown in Fig. 1, and are connected to FS-N11MN Fiber Optic Sensor, by Keyence Co., Ltd. The Keyence optic sensor has two light channels, one for emitting and for receiving light. The device works both as a light source and receiver of the reflected light, and eventually converts the amount of reflective light into voltage. When an external force is applied on the upper plate, three cantilever beams will be deformed as shown in Fig. 3. The three pairs of optical fibers can measure deformations δ_1, δ_2, and, δ_3 on the three points between the upper plate and the bottom plate as shown in Fig. 3. In order to anchor the force sensor to the structure of the STIFF-FLOP manipulator, a click-on mechanism is adopted, as shown in Figs. 1 and 2. The ring-like, hollow sensor structure allows passing optical fibers between the arm segments and connecting them to the force sensor.

C. Sensor Structure Design and Simulation

To measure the force/moment components, three cantilever beams are used as shown in Fig. 3. To satisfy the force range requirements of the STIFF-FLOP manipulator (0-10 N), we have performed an FEM analysis. Fig. 4 shows the result of the FEM simulation by using the SolidWorks Simulation tool, revealing that the sensor can measure the force within the required range. The material property values in this simulation were set at: tensile modulus of 1283 MPa, mass density of 1020 kg/m^3, yield strength of 42500000 N/m^2; these assumptions were based on information provided by PROJET VisiJet® EX200, 3D SYSTEM Co., Ltd.

D. Optimization of Deployment of Optical Fibers

In order to develop an optical based force sensor, the following key points should be considered: (1) a small deformation resulting from an external force should produce a sufficiently large value for the output voltage of the fiber optic sensor; (2) the output voltage of the fiber optic sensor should change linearly with respect to distance between optical fibers and the mirror, to lead to a linear relationship between physical force and output voltage of the optical fiber.

However, depending on the distance from the mirror to the tips of the fibers, the orientation angle between two optical fibers a, and the depth d between them, the characteristic curve between the output voltage of the optical fiber and the distance was found to be different (Fig. 5). For this reason, in order to satisfy the two key points for the development of the optical force sensor, a device is proposed to optimize the measured voltage values against the corresponding actual parameters, including depth d and angle a. Using this device, the optimized angle between the two optical fibers has been determined as follows:

1) Experiment for Optimization of Deployment of Optical Fiber

1.1) Device Design

The device consists of a mirror, a linear guide, an actuator, and a rotational unit, which can adjust an amount of angle and distance between the two optical fibers as shown in Fig. 6. The actuator moves in a translational direction along the linear guide and the characteristic curve is obtained as shown in Figs. 7, 8 and 9. The characteristic curve shows how much the measured optical fiber voltages change with respect to distance. This device, ADC (Analog to Digital Convertor), and software can obtain characteristic curves between output voltage of the optical fiber and distance (actuator's encoder data).

1.2) Setup for Experiments

The angle between an optical fiber pair and the distance between their tips and the mirror are adjusted as shown in Fig. 6: this is achieved by changing angle a and depth d, namely the distance between the mirror and the two optical fibers along the linear guide using DC motor.

As shown in Figs. 5 and 6, the distal part of the two optical fibers was adjusted to be 6.5 mm away from the mirror. Then, a profile of different angles a (0°, 15°, and 30°) and different depths d (1, 2, 3) were tested while the distance between the fibers and the mirror were modulated from 0 mm to 6 mm along the linear guide, Figs. 5 and 6. In this way, the characteristic curve between the output voltage of the optical fiber and the distance between the mirror and the two optical fibers was obtained.

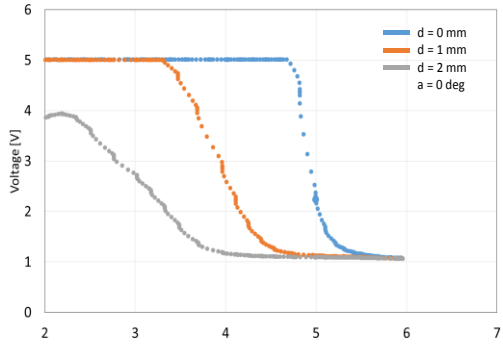

Figure 7. Characteristic curve of output voltage of optical fiber in case of a = 0°and changing d

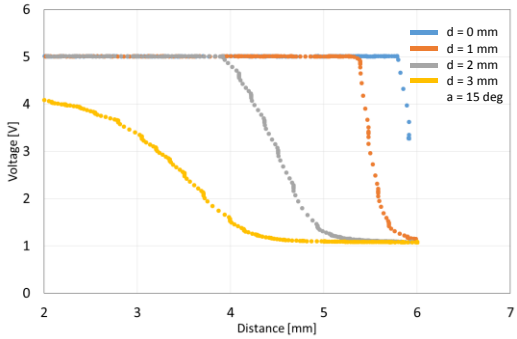

Figure 8. Characteristic curve of output voltage of optical fiber in case of a = 15°and changing d

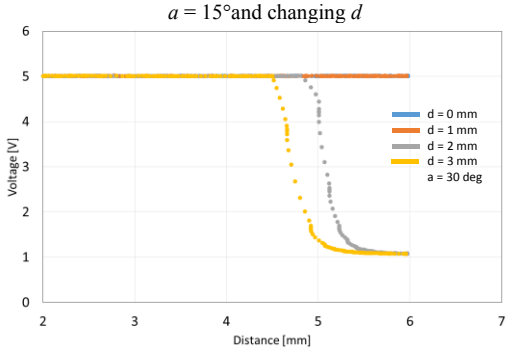

Figure 9. Characteristic curve of output voltage of optical fiber in case of a = 30°and changing d

1.3) Experimental Results

Fig. 7 shows profiles of output voltage versus the distance to the mirror when a = 0°, and at three different depths d. It can be seen that in the vicinity of the mirror, the output voltage of the optical fiber suddenly changes from 1 V to 5 V. For smaller values of depth d, the output voltage of the optical fiber demonstrated a sharp nearly linear change in the vicinity of the mirror, and so the linearity was improved. As shown in Figs. 8 and 9, in case of adjusting angles a, depths d, the output voltage of the optical fiber changes from 1 to 5 V. The smaller depths d accompanied with bigger values of angles a result in a better linearity of the voltage-distance profile. Note that in Fig. 9, the voltage change was not observed at around 6 mm away from the mirror, since the output voltage of the two optical fibers was in the saturated region.

1.4) Discussion on the Experiments

From the results of the experiments, the design of the three axis sensor can be attempted. In order to satisfy the three conditions of the force sensor development, the characteristic curve d = 1 and a = 15° (orange curve) can be used as shown in Fig. 8 providing sufficient linearity and producing a 4 V change in response to 0.5 mm distance change. Although the other curves also potentially provide good possibilities for the design, their characteristic curves are highly non-linear, and are too steep with respect to tiny distances, causing the output voltage to be saturated easily.

III. Sensor Calibration

A. Sensor Calibration

In order to use a self-fabricated sensor prototype as a force sensor, calibration is required. The calibration process aims at obtaining a relationship between the output voltages of the optical fiber and physical force F_z and physical moments M_x and M_y. For this reason, we propose a calibration device and calculated coefficients of linear fitting function for a proper prediction of the applied force and momentum components from the calibration data.

1) Calibration Device

The calibration device consists of a base, a sensor fixture, and a load fixture. For the calibration, the developed three axis force sensor was attached to the calibration device as shown in Fig. 10. For F_z calibration, the load fixture is attached to the sensor fixture as shown in the same figure, whereas in the cases of M_x and M_y calibration, another type of load was attached on the sensor fixture as shown in Figs. 11 and 12. This calibration device also uses an Analogue-Digital Converter (ADC) and its associated software to obtain the characteristic curves between the output voltage of the optical fibers and the physical load.

2) Calibration for Force Components

As shown in Fig. 10, loads - in the range from 0 N to 7 N - were attached to the load fixture, and the characteristic curve between the loads F_z and the output voltage of the force sensor were obtained. The loads lead to output voltages for the three optical fibers in the region of 2.5 V, in Fig. 13. It is noted that the three characteristic curves are not completely linear.

Referring to the moment calibration in Fig. 11, loads from 0 Ncm to 3.5 Ncm were attached to the load fixture, and the characteristic curves between the loads M_x and the output voltage of the three optical fibers were obtained. The loads lead to fiber output voltages as shown in Fig. 14. Even in this case, the characteristic curves are not completely linear.

Similarly, in Fig. 12, loads from 0 Ncm to 3.5 Ncm were attached to the load fixture, and the characteristic curve between the loads M_y and the output voltage from the three optical fibers were computed (Fig. 15). As it is shown, the characteristic curves are not perfectly linear.

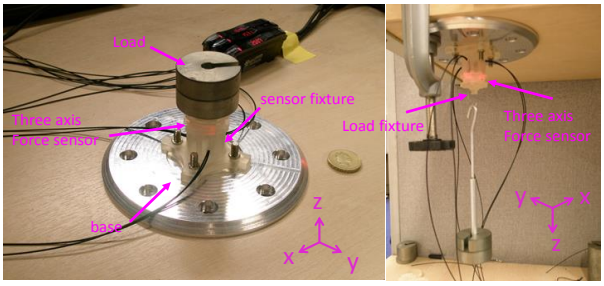

Figure 10. Experimental set-up for the calibration of F_z

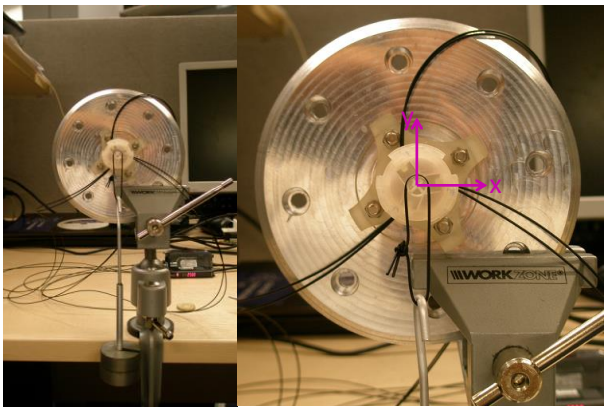

Figure 11. Calibration method for M_x

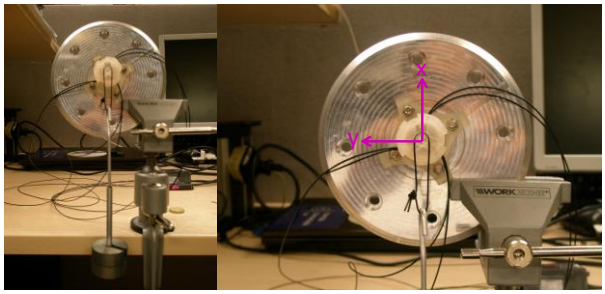

Figure 12. Experimental set-up for the calibration of M_y

B. *Calculation of Force Components by Multiple Linear Regression*

Multiple linear regression aims at finding the relationship between two or more variables and a response variable by means of fitting a linear equation to the observed data [20]. In this implementation, every value of an independent variable - namely each value of the three output voltage of the optical fibers - is associated with values of the dependent variables - namely the force F_z, and the moments M_x, and M_y.

By applying the multiple linear regression, F_z, M_x and M_y can be calculated from the three sensor voltage samples V_1, V_2, and V_3, as shown in Eq. (1) to (3). According to this calculation, the estimated F_z, M_x and M_y differ from the real F_z, M_x, and M_y, as shown in Fig. 16 to 18. Particularly, M_x has some error when compared with the other errors of F_z and M_y (Fig. 17 and Table 1):

$$Fz = -0.103V_1 + 1.724V_2 + 3.836V_3 \quad (1)$$
$$Mx = -31.807V_1 - 4.670V_2 + 67.319V_3 \quad (2)$$
$$My = -2.516V_1 - 0.949V_2 + 0.849V_3 \quad (3)$$

TABLE I. SENSOR ERROR PROPERTY

Force / Moment	Range	Maximum error
Fz	+/- 6 [N]	0.255 [N] (2.1%)
Mx	+/- 3.5 [Ncm]	0.996 [Ncm] (14.2%)
My	+/- 2.5 [Ncm]	0.216 [Ncm] (3.0%)

IV. CONCLUSION AND FUTURE WORKS

In this paper, we have presented details of an optical based three axis force sensor used to measure external forces applied to the STIFF-FLOP manipulator. We have demonstrated how to design a sensor structure which enables multi axis sensing in a multi-segment soft manipulator and optimized the deployment (relative orientation) of the two optical fibers in order to obtain maximum sensing range. In addition, we proposed how to calibrate the sensor and calculate the force components of the sensor to estimate the applied force and momentum components employing multiple linear regression. Finally, we have also validated the effectiveness of our

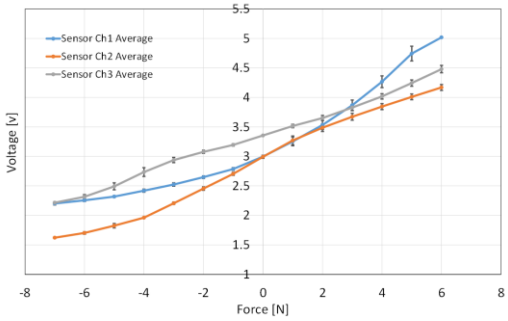

Figure 13. Characteristic curve between the loads F_z, and the output voltage of the force sensor

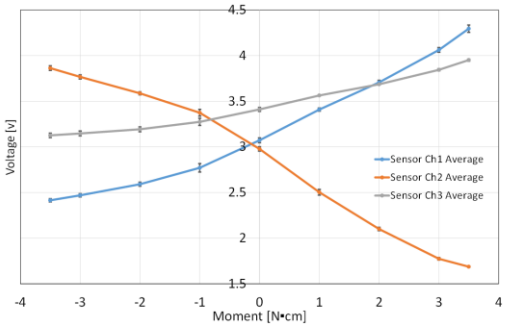

Figure 14. Characteristic curve between the loads M_x, and the output voltage of the force sensor

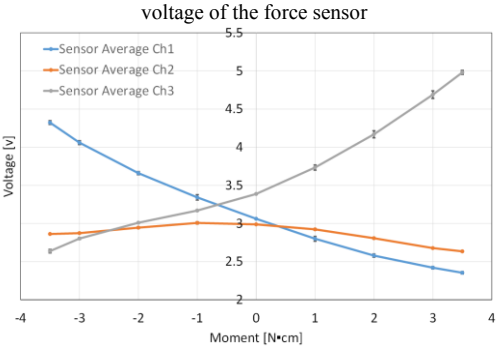

Figure 15. Characteristic curve between the loads M_y, and the output voltage of the force sensor

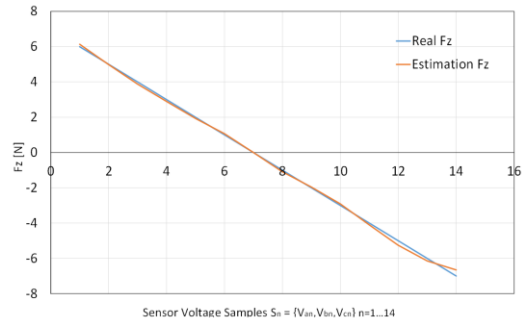

Figure 16. Comparison between real values and linear regression estimation of F_z

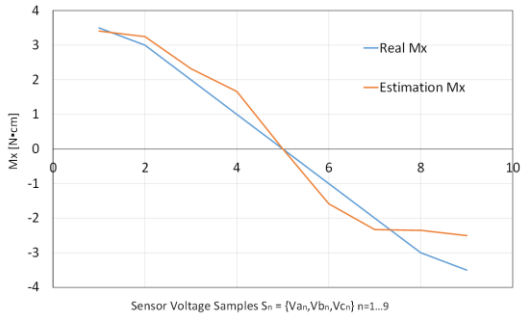

Figure 17. Comparison between real values and linear regression estimation of M_x

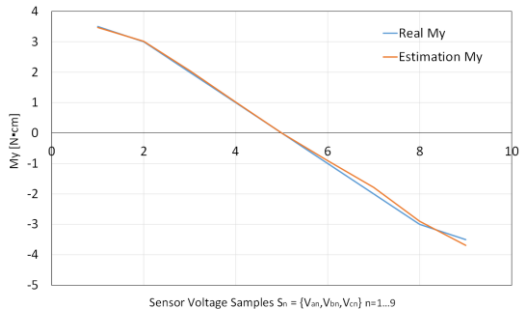

Figure 18. Comparison between real values and linear regression estimation of M_y

proposed three axis force sensor through a set of experiments.

As a future task, the deployment of pairs of optical fibers should be optimized to achieve higher sensor linearity (to reduce the sensor error as shown in Table 1), and to evaluate and improve sensor characteristics such as error, nonlinearity, crosstalk, repeatability, and hysteresis. In addition, our proposed three axis force sensor will be integrated within the STIFF-FLOP manipulator in order to measure external force and momentum components. As the hysteresis level of the multi-axis sensor proposed in this study is high, we aim to use MRI compatible metals such as titanium, aluminium for future sensors, instead of the currently used ABS plastic.

REFERENCES

[1] W. Reynolds, "The First Laparoscopic Cholecystectomy", JSLS 5:89-94, 2001.

[2] A. Rané, G. Y. Tan, and A. K. Tewari, "Laparoendoscopic single-site surgery in urology: is robotics the missing link?", BJU International, 2009; pp. 1041–1043.

[3] N. Simaan, K. Xu, A. Kapoor, W. Wei, P. Kazanzides, P. Flint, and R. Taylor, "A System for Minimally Invasive Surgery in the Throat and Upper Airways", Int. J. Robotics Research (special issue on medical robotics), vol. 28- 9, pp. 1134-1153, June 2009.

[4] Alexander T. Hillel, Ankur Kapoor, Nabil Simaan, Russell H. Taylor and Paul Flint, " Applications of Robotics for Laryngeal Surgery," Laryngeal Cancer -Otolaryngologic Clinics of North America, Nasir Bhatti & Ralph P. Tufano Eds., Volume 41, Issue 4, Pages 781-791, August 2008.

[5] Zhang, J., Bhattacharyya, S., Simaan, N., "Model and Parameter Identification of Friction During Robotic Insertion of Cochlear-Implant Electrode Arrays," IEEE International Conference on Robotics and Automation (ICRA'2009), pp. 3859-3864, 2009.

[6] Zhang, J., Wei, W., Roland, J., Manolidis, S., Simaan, N., "Optimal Path Planning for Robotic Insertion of Steerable Electrode Arrays in Cochlear Implant Surgery", in ASME Journal on Medical Devices, Vol 3., No. 1, pp. 011001, 2009.

[7] D. C. Rucker, B. A. Jones, and R. J. Webster III. A Geometrically Exact Model for Externally Loaded Concentric Tube Continuum Robots. IEEE Transactions on Robotics, 26(5), 769-780, 2010.

[8] D. C. Rucker, R. J. Webster III, G. S. Chirikjian, and N. J. Cowan. Equilibrium Conformations of Concentric-Tube Continuum Robots. International Journal of Robotics Research, 29(10), 1263-1280, 2010. (Pre-typesetting preprint) Final definitive version available from IJRR.

[9] N.G. Cheng, M.B. Lobovsky, S.J. Keating, A.M. Setapen, "Design and Analysis of a Robust, Low-cost, Highly Articulated manipulator enabled by jamming of granular media", The 2012 IEEE International Conference on Robotics and Automation (ICRA), pp. 4328 – 4333, 2012

[10] A Jiang, G Xynogalas, P Dasgupta, K Althoefer, T Nanayakkara,"Design of a variable stiffness flexible manipulator with composite granular jamming and membrane coupling", 2012 IEEE/RSJ International Conference on Intelligent Robots and Systems (IROS 2012), pp. 2922 – 2927, 2012

[11] A Jiang, A Ataollahi, K Althoefer, P Dasgupta, T Nanayakkara, "A Variable Stiffness Joint by Granular Jamming", Proceedings of the ASME 2012 International Design Engineering Technical Conference & Computers and Information in Engineering Conference (IDETC 2012)

[12] Tommaso Ranzani, Matteo Cianchetti, Giada Gerboni, Iris De Falco, Gianluigi Petroni, Arianna Menciassi," A modular soft manipulator with variable stiffness," 3rd Joint Workshop on New Technologies for Computer/Robot Assisted Surgery Sept 2013, Verona, Italy

[13] M. Cianchetti, T. Ranzani, G. Gerboni, C. Laschi, A. Menciassi," Preliminary mechanical design of a soft manipulator for minimally invasive surgery", 2013 International Workshop on Soft Robotics and Morphological Computation pp. 23, 2013

[14] Matteo Cianchetti, Tommaso Ranzani, Giada Gerboni, Iris De Falco, Cecilia Laschi, Arianna Menciassi,"STIFF-FLOP Surgical Manipulator: mechanical design and experimental characterization of the single module", IEEE/RSJ 2013 International Conference on Intelligent Robots and Systems, pp. 3576-3581, 2013

[15] Thomas C. Searle, Kaspar Althoefer, Lakmal Seneviratne, Hongbin Liu," An Optical Curvature Sensor for Flexible Manipulators", The 2012 IEEE International Conference on Robotics and Automation (ICRA 2012), pp. 4401 – 4405, 2012

[16] P Polygerinos, P Puangmali, T Schaeffter, R Razavi, LD Seneviratne, "Novel miniature MRI-compatible fiber-optic force sensor for cardiac catheterization procedures", The 2010 IEEE International Conference on Robotics and Automation (ICRA 2010), pp. 2598 – 2603, 2010

[17] P Puangmali, H Liu, LD Seneviratne, P Dasgupta, K Althoefer, "Miniature 3-axis distal force sensor for minimally invasive surgical palpation", Mechatronics, IEEE/ASME Transactions on 17 (4), 646-656

[18] Panagiotis Polygerinos, Dinusha Zbyszewski, Tobias Schaeffter, Reza Razavi, Lakmal D Seneviratne, Kaspar Althoefer," MRI-compatible fiber-optic force sensors for catheterization procedures", IEEE Sensors Journal, pp. 1598-1608, 2010

[19] H. Liu, J. Li, X. Song, L. D. Seneviratne, K. Althoefer, "Rolling indentation probe for tissue abnormality identification during minimally invasive surgery", IEEE Transactions on Robotics, 27(3), 450-460, 2011

[20] Laura L. Nathans, Frederick L. Oswald, Kim Nimon, "Interpreting Multiple Linear Regression: A Guidebook of Variable Importance", Practical Assessment, Research & Evaluation, Vol. 17, No. 9